# Lipidic Sponge Phase Crystallization of Membrane Proteins

**ARTICLE** *in* JOURNAL OF MOLECULAR BIOLOGY · DECEMBER 2006

Impact Factor: 4.33 · DOI: 10.1016/j.jmb.2006.06.043 · Source: PubMed

doi:10.1016/j.jmb.2006.06.043 J. Mol. Biol. (2006) 364, 44–53

JMB

Available online at www.sciencedirect.com

ScienceDirect

ELSEVIER

# Lipidic Sponge Phase Crystallization of Membrane Proteins

**Pia Wadsten[1], Annemarie B. Wöhri[2], Arjan Snijder[2] Gergely Katona[3], Alastair T. Gardiner[4], Richard J. Cogdell[4] Richard Neutze[2]* and Sven Engström[1]**

[1]*Department of Chemical and Biological Engineering Pharmaceutical Technology Chalmers University of Technology, SE-412 96 Göteborg, Sweden*

[2]*Department of Chemical and Biological Engineering Molecular Biotechnology Chalmers University of Technology, SE-405 30 Göteborg, Sweden*

[3]*LCCP, UMR 9015 IBS-CEA/ CNRS/Université J. Fourier, 41 Avenue Jules Horowitz, 38027 Grenoble, Cedex 1, France*

[4]*Division of Biochemistry and Molecular Biology, Institute of Biomedical and Life Sciences University of Glasgow, Glasgow G12 8QQ, Scotland, UK*

**Corresponding author*

Bicontinuous lipidic cubic phases can be used as a host for growing crystals of membrane proteins. Since the cubic phase is stiff, handling is difficult and time-consuming. Moreover, the conventional cubic phase may interfere with the hydrophilic domains of membrane proteins due to the limited size of the aqueous pores. Here, we introduce a new crystallization method that makes use of a liquid analogue of the cubic phase, the sponge phase. This phase facilitates a considerable increase in the allowed size of aqueous domains of membrane proteins, and is easily generalised to a conventional vapour diffusion crystallisation experiment, including the use of nanoliter drop crystallization robots. The appearance of the sponge phase was confirmed by visual inspection, small-angle X-ray scattering and NMR spectroscopy. Crystals of the reaction centre from *Rhodobacter sphaeroides* were obtained by a conventional hanging-drop experiment, were harvested directly without the addition of lipase or cryoprotectant, and the structure was refined to 2.2 Å resolution. In contrast to our earlier lipidic cubic phase reaction centre structure, the mobile ubiquinone could be built and refined. The practical advantages of the sponge phase make it a potent tool for crystallization of membrane proteins.



*Keywords:* protein crystallization; sponge phase; reaction centre from *Rhodobacter sphaeroides* (RCsph); lipid phase transitions; monoolein (MO)

## Introduction

Approximately 20–30 % of the genes in the human genome code for integral membrane proteins, which have a variety of essential functions, such as signal transduction, transport, and charge separation. Detailed structural information is required to fully understand these fundamental processes. Protein crystallography has proven to be the most productive method for studying the structural biology of membrane proteins. Nevertheless, the preparation of well-diffracting crystals remains a major bottleneck, particularly for membrane proteins. According to the membrane protein resources homepage†, there are currently 113 structures of unique membrane proteins.

Membrane proteins are native to a lipidic environment, while protein crystallization techniques were developed with aqueous solutions in mind. Crystallization methods for membrane proteins are based upon detergent-solubilized protein being crystallized by standard methods such as vapour-diffusion crystallization.[1] In 1996, Landau & Rosenbusch

Abbreviations used: MO, monoolein; SAXS, small-angle X-ray scattering; LCP, lipidic cubic phase; PEG, polyethylene glycol; PG, propylene glycol; MPD, 2-methyl-2,4-pentanediol; DMSO, dimethyl sulfoxide; PPO, pentaerythritol propoxylate; NMP, *N*-methylpyrrolidinone; RC, reaction centre; RCsph, reaction centre from *Rhodobacter sphaeroides*.

E-mail address of the corresponding author: richard.neutze@chembio.chalmers.se

† http://blanco.biomol.uci.edu/Membrane_Proteins_xtal.html

introduced a new crystallization method that offers a lipidic environment (cubic phase) to the protein.[2] The cubic phase was made of a mixture of monoolein (MO) and water, which forms two bicontinuous cubic phases in the presence of an excess of water (symmetry Ia3d and Pn3m, respectively). Their bicontinuous structure was established in the early 1980s by a combination of small-angle X-ray scattering (SAXS) and NMR diffusion measurements.[3–5] Crystals grown in the lipidic cubic phase (LCP) are arranged as stacked 2D bilayers,[6] have been rather robust, of high quality and often superior to detergent-grown crystals. Unique crystal structures obtained by this method so far are bacteriorhodopsin,[7–9] halorhodopsin,[10] sensory rhodopsin II,[11,12] sensory rhodopsin II with the transducer complex,[13] *Anabaena* sensory rhodopsin,[14] the reaction centre from *Rhodopseudomonas virdis*,[15] the reaction centre from *Rhodobacter sphaeroides*[6] and BtuB.[16] Furthermore, the membrane proteins are typically active within LCP-grown crystals. For example, functionally relevant light-induced relative movements have been seen in bacteriorhodopsin[17–21] sensory rhodopsin II[22,23] and the reaction centre from *Rhodobacter sphaeroides*.[24]

The crystallization process in the LCP has been a matter of discussion. It is frequently argued that the saddle-shaped bicontinuous lipid bilayer of the cubic phase facilitates protein diffusion, which is a prerequisite for nucleation and growth of crystals. Nevertheless, since the cubic phase is highly curved with a relatively small inner pore, this may make it difficult to host a membrane protein with larger hydrophilic domains. In order to make it easier for the protein to diffuse in the lipid bilayer, it can be flattened out by various means. One way is to reduce the water content of the cubic phase, since the MO/water system undergoes a phase transformation from a curved Pn3m cubic phase, *via* a less curved Ia3d cubic phase, to a flat lamellar phase ($L_\alpha$).[25] Secondly, one could instead flatten the bilayer curvature by adding charged lipids or amphiphiles to the system and subsequently widen the water pores.[26,27]

A third alternative is to use solvents or other additives such as polyethylene glycol (PEG), propylene glycol (PG), ethanol, 2-methyl-2,4-pentanediol (MPD), dimethyl sulfoxide (DMSO), pentaerythritol propoxylate (PPO), *N*-methylpyrrolidinone (NMP), butanediol, jeffamine, KSCN or t-butanol, to the binary MO/water system in order to create a sponge phase ($L_3$- phase).[28–31] Specifically, this bicontinuous phase is a transparent liquid with an inner structure that may be visualized as a "melted" cubic phase with a less curved lipid bilayer and two to three times larger aqueous pores.[32] In this work, we show that the reaction centre from *Rhodobacter sphaeroides* (RCsph) can be crystallized directly from a sponge phase in an ordinary hanging-drop experiment. Our hypothesis that RCsph crystallized from a sponge phase was confirmed by visual inspection, SAXS and NMR data. There are several specific advantages of the sponge phase over the more conventional LCP and, in particular, the crystallization methods widely used by the structural biology community, such as vapour-diffusion crystallization, automation, and standard optimization protocols can be applied directly.

## Results and Discussion

### Characterization of the sponge phase during RCsph crystal growth

In the standard LCP crystallization method, described by Landau & Rosenbush, MO is mixed with the protein in aqueous solution; the resulting protein-containing cubic phase is then placed in contact with precipitant solution.[2] In such crystallization setups, precipitant solutions often contain substances that lead to phase transformations in the MO/water system.[33] This mechanism has been elaborated upon by further studies.[34] Another crystallization approach reminiscent of this concept is the bicelle crystallization protocol, which also implicates phase transformation.[35] A third example of crystal growth during a phase transformation is the crystallization process of RCsph from the LCP. In previous work, we obtained 3D crystals of RCsph from the LCP of the type I stacked bilayer form in the presence of jeffamine M600, 1,2,3-heptanetriol and $(NH_4)_2SO_4$.[6] By visual inspection, these setups appeared to liquefy, indicating a phase transformation. This observation prompted a deeper characterization of the phase transformation and its influence on the crystal quality.

A series of experiments were performed to characterize the crystallization process from the LCP. Our simplest characterization was to add crystal violet to a cubic phase without protein. Crystal violet is known to accumulate at lipid/water (detergent/water) interfaces, such as the MO/water interface in the cubic phase.[36] After addition of precipitant solution, the semi-solid cubic phase started to transform and was gone after approximately 20 h, resulting in two liquid phases (upper/lower) in the test-tube (Figure 1). Crystal violet was observed in the upper liquid phase, indicating that most of the MO has moved into this phase and most probably in the form of a self-assembled structure due to its low solubility in water. This conclusion was confirmed using $^1H$ NMR ($^2H_2O$), which showed large amounts of MO together with jeffamine M600 in the upper phase, while the lower phase contained only trace amounts of jeffamine M600 and MO (data not shown). That MO migrates from the bottom to the top of the test-tube is due to the fact that the original cubic phase, which is less dense than the screen solution, sticks to the glass wall and is prevented from floating to the top of the screen solution.

SAXS was used to examine the phase transformation from LCP to a liquid under conditions identical with those used for a crystallization experiment but without protein. The LCP was transferred into a capillary, precipitant solution was added from both

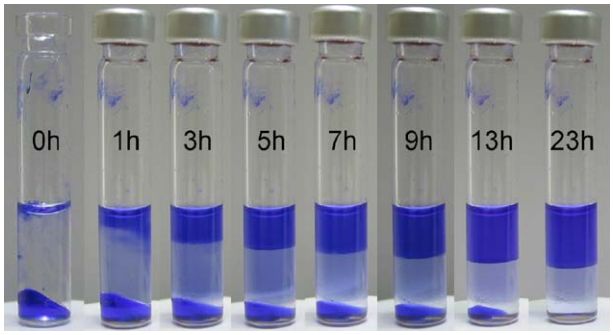


**Figure 1.** Phase separation visualized by crystal violet. The initially two-phase system composed of lipidic cubic phase and crystallization agent evolves into a three-phase system containing a cubic phase and two liquid phases (1–13 h). After approximately 20 h, the cubic phase is totally dissolved and two liquid phases are observed. Crystal violet (blue) moves to the lipid-rich partition.

sides, and the capillary was placed into the diffractometer. The sample was measured every 30 min for 5 min over a period of 16 h. Initially, the predominant X-ray scattering peak position corresponded to a cubic phase with Pn3m symmetry. After 5 h, an additional diffraction pattern with space symmetry Ia3d appeared in the diffractogram; after 8 h the Pn3m pattern had disappeared and only the Ia3d pattern remained. This Ia3d pattern disappeared after 10 h and was replaced by a relatively broad Bragg peak closer to the primary beam. We interpret the Ia3d pattern as originating from a cubic structure, and the diffuse Bragg peak as resulting from the formation of an $L_3$ or sponge phase (Figure 3(a)). The lattice parameter obtained for the Ia3d structure in the SAXS capillary is considerably larger than that obtained for the most swollen MO/water cubic phase with Ia3d symmetry (160 Å at 20 °C).[37] The two liquid phases that formed after 24 h (Figure 1) were investigated by SAXS, and their diffractograms are given in Figure 3(b) (a diffraction pattern obtained for the original Pn3m cubic phase is also shown for comparison). The lower phase had no characteristic scattering pattern indicating a lack of ordered structure that can be accounted for by the very small amounts of MO in this phase. The upper phase, however, showed a broad Bragg peak with its maximum at about $q_{max} = 0.025$ Å$^{-1}$, revealing a distance $d = 255$ Å ($d = 2\pi/q_{max}$). This value is within the range characteristic for other sponge phases.[38,39] The lattice parameters of a sponge phase made with jeffamine were reported recently.[31] Finally, when the upper phase was stored at 4 °C for a week, it was transformed to a birefringent lamellar phase. Since the sponge phase responds dynamically to changes of temperature and forms a lamellar phase when the temperature is decreased, this supports the hypothesis that the upper phase is a sponge phase.[40]

## Crystallization of RCsph in a sponge phase using the vapour-diffusion technique

In the previous section we established that a transition from a cubic to a sponge phase occurs under the LCP crystallization conditions used for RCsph. Since this sponge phase is liquid, it was used directly in a standard vapour–diffusion, hanging-drop experiment. Our approach was to mix four parts of the sponge phase with one part of concentrated protein solution. Crystals formed after one week (Figure 2) within the pH range of 7.5 to 9.2, and with a concentration of jeffamine M600 above 5% (v/v). As a control, identical setups were performed without jeffamine M600, but no $L_3$ phase was formed and hence no crystal was obtained. These crystals displayed a morphology different from that of the previous LCP RCsph crystals and other LCP-grown crystals, which were typically observed as thin plates. In particular, the new crystals are larger and roughly equal in all dimensions. After two weeks the

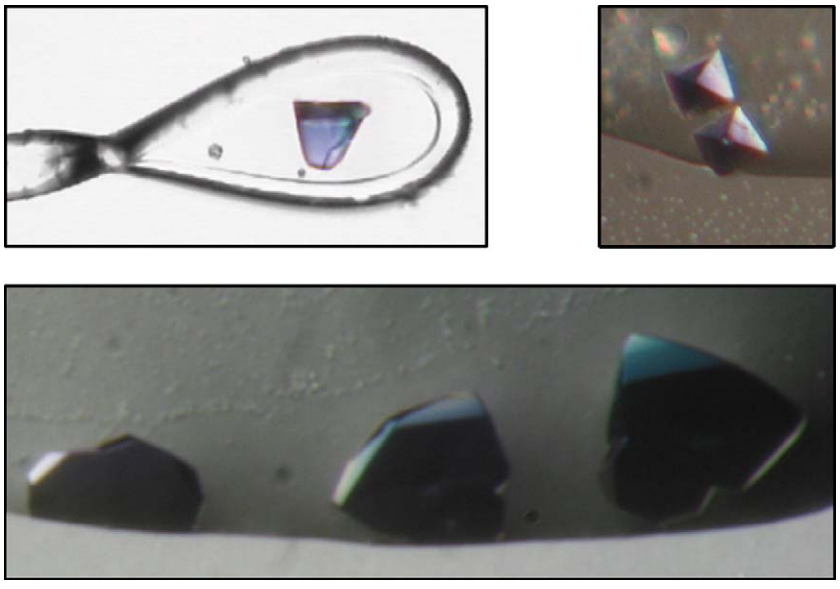

**Figure 2.** Crystals grown directly from the $L_3$ phase using MO and buffer solution. (a) RC crystal fished directly from the $L_3$ phase. (b) and (c) Crystals of RC grown in 20% jeffamine M600 (pH 8.1).

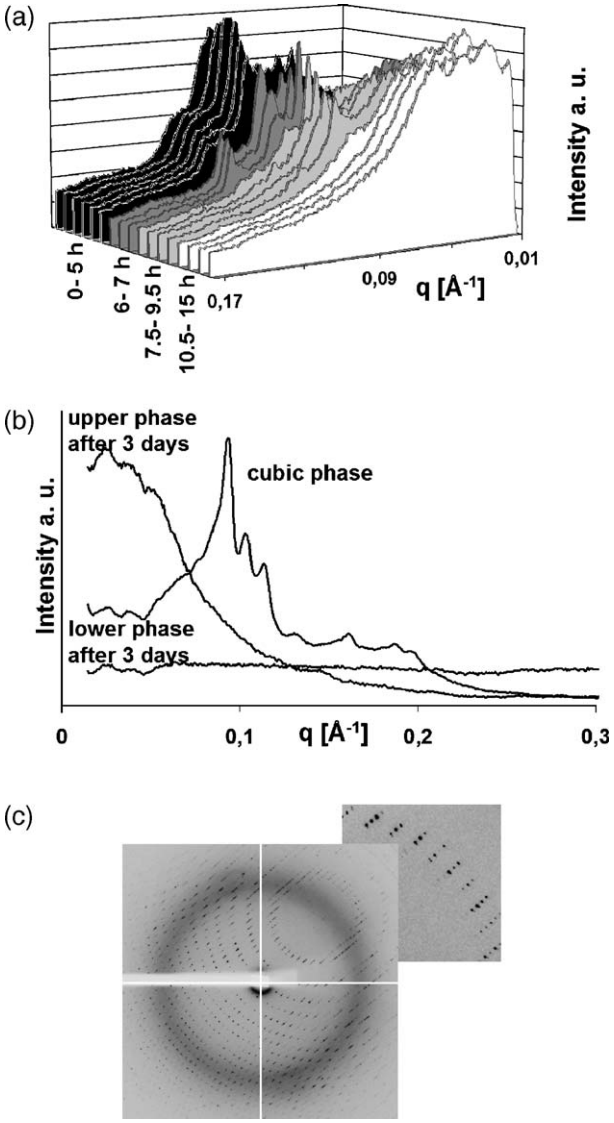


**Figure 3.** SAXS measurement at 20 °C. (a) Phase transformation (cubic to sponge) after addition of a crystallization agent containing 20% jeffamine M600. (b) Upper and lower liquid phases measured after three days. The fully swollen cubic liquid crystalline phase (Pn3m) is shown for comparison. (c) Diffraction pattern of RCsph: $\lambda = 0.933$ nm; sample to detector distance 180 mm; exposure time 10 s; oscillation 0.5°.

crystals were harvested directly from the sponge phase without addition of lipase or cryoprotectants. This represents a practical advantage over the fishing procedure with LCP, which frequently requires lipase to hydrolyse the monacylglycerols,[41] otherwise it is difficult to extract crystals from the semi-solid LCP.

Mounted and frozen crystals were used for X-ray diffraction measurements at beam-line ID14/EH2 of the European Synchrotron Radiation Facility (Grenoble, France). Diffractions spots were observed to 1.9 Å (Figure 3c), but data could be processed to only 2.2 Å because of the low signal-to-noise ratio ($I/\sigma$). The crystals were isomorphic with the LCP RCsph crystals belonging to space group $P4_22_12$, with one molecule per asymmetric unit and the molecules are arranged within stacked anti-parallel planes.[6] Entry 1OGV[6] of the Protein Data Bank was used as a starting model for the refinement[6] and, after simulated annealing and iterative rounds of refinement, the $R$-factor was 20.0% and the $R_{free}$ was 24.6%. Structural analysis using internal distance matrixes with the program ESCET[42] showed no significant structural differences, with 99.7% identity with the model 1OGV.[42] The crystallographic data and final refinement statistics are summarized in Table 1.

Because of the improved resolution and better data quality, the electron density from a simulated-annealing omit map ($2F_o - F_c$) omitting ubiquinone ($Q_B$) showed a strong positive signal in the binding pocket (Figure 4(c)). This significant improvement made it possible to model ubiquinone at the $Q_B$ binding pocket with two isoprenic units for the tail (Figure 4(b)). The exact conformation of the mobile $Q_B$ has been an issue of considerable debate within the literature, with 32 PDB entries all showing significant variation in the position of $Q_B$. In Figure 4(d) we overlay our $Q_B$ binding site (orange) with a representative set of four other RC structures.[43–45] Of the 32 deposited structures, only one other structure 1YST (red)[43] has the same orientation for the $Q_B$ head group as we recover (orange). For example, when compared with the structure of the light-adapted RCsph (light green),[45] the head group of $Q_B$ is displaced by 0.7 Å away from the binding pocket and consequently is buried less deeply within the protein. Relative to the dark-adapted structure (dark green) from the same publication, our head-group of $Q_B$ (orange) is displaced 3.6 Å into the binding pocket. The head-group of another representative structure, 1RG5 (blue),[44] appears to be buried even more deeply than ours (orange) and the light-adapted structure (light green).

Structural comparison of the ubiquinone tail shows that the $Q_B$ tail packs tightly against the protein in all 32 PDB entries, and that these may be divided into two main groups: those with the tail packed against the transmembrane regions of the M subunit; and those with the tail packed against the hydrophobic/hydrophilic membrane interface near the H subunit. Our structure appears to lie somewhere between these two categories, with a kink in the tail orienting it towards the open space occupied by the native membrane (Figure 4(a)). In particular, the second isoprenic unit of the $Q_B$ tail is displaced approximately 3.5 Å away from the protein relative to all other structures of $Q_B$. When $Q_B$ is fully reduced by two turnovers of the RC, it leaves the RC-binding pocket and delivers its reducing equivalents to the cytochrome $bc_1$ complex. From its functional role, it is not surprising that different RC crystal structures show $Q_B$ in different positions. Nevertheless, since we have crystallized the RCsph as a stacked bilayer in a type I crystal form using MO as a host for the protein, the native membrane is substituted by lipid molecules in these crystals. It is therefore plausible that the electron density we

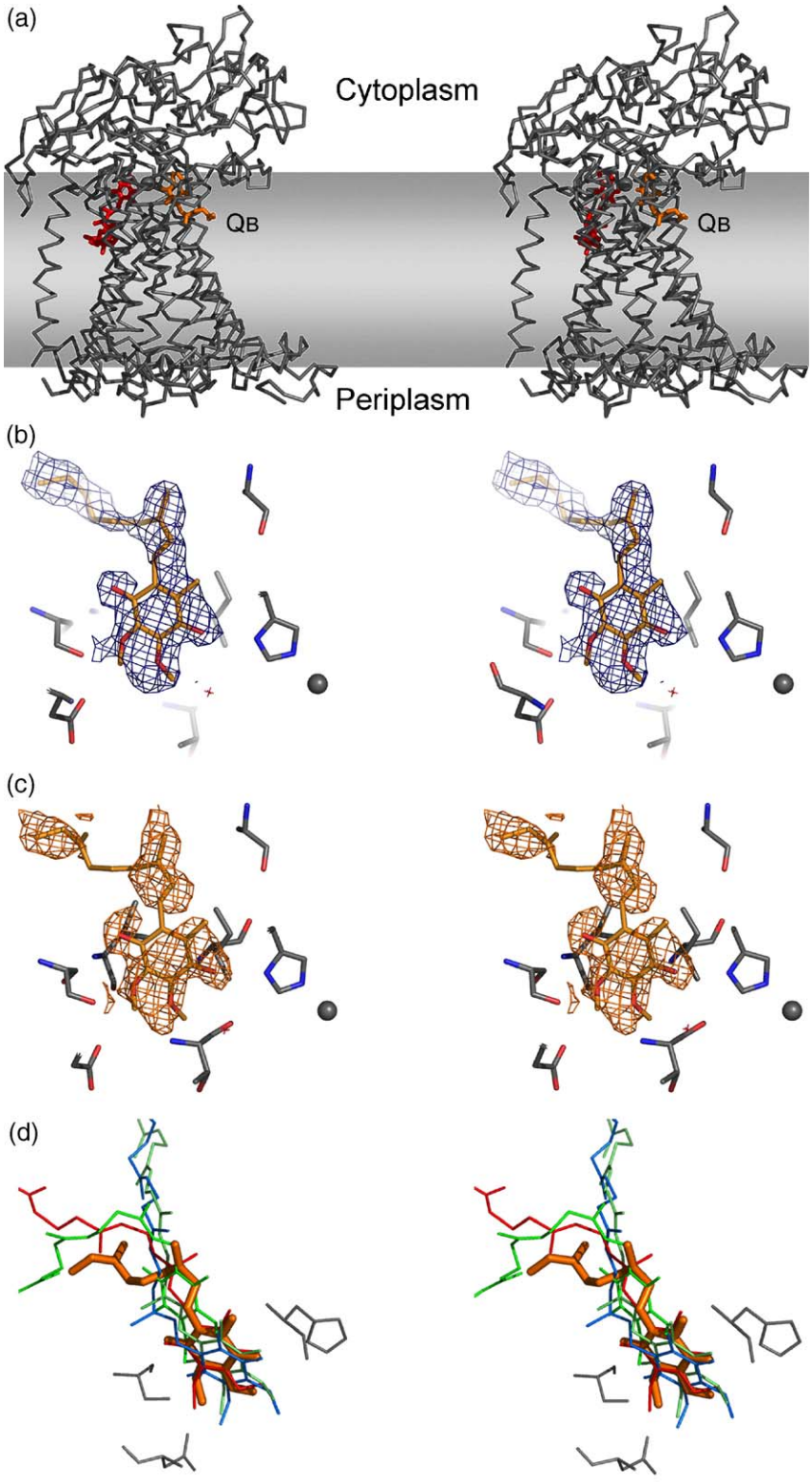


**Figure 4.** $Q_B$ binding sites of RCsph. All pictures are represented in stereoview. (a) Arrangement of the cofactors $Q_A$ and $Q_B$, subunits H, L, M and the location of the membrane in RCsph. The colouring scheme is: H, L, M subunit (dark grey), cofactors $Q_A$ (red), $Q_B$ (orange). The approximate position of the membrane is indicated by the light grey square. (b) Refined electron density for the $Q_B$ binding pocket. The $2F_o - F_c$ map is contoured at 1σ. (c) Simulated-annealing omit map omitting $Q_B$ contoured at 1σ. (d) Superposition of ubiquinone in the $Q_B$ binding pocket. Colour code and PDB entries: red, 1YST;[43] light green, 1AIG;[45] dark green, 1AIJ;[45] blue, 1RG5;[44] orange, present structure 2GNU.

**Table 1.** Crystallographic data and refinement statistics

| | | | | |
|---|---|---|---|---|
| Resolution (Å) | 52.63–2.20 (2.32–2.20) | | | |
| No. unique reflections | 61,848 | | | |
| Completeness (%) | 99.8 (100) | | | |
| Multiplicity[a] | 10.2 (4.9) | | | |
| Mosaicity (deg.) | 0.5 | | | |
| $\langle I/\sigma \rangle$[a] | 5.6 (0.9) | | | |
| $R_{sym}$ (%)[a,b] | 11.7 (64.1) | | | |
| $R$ (%)[c] | 20.0 | | | |
| $R_{free}$ (%)[c] | 24.6 | | | |
| r.m.s. bond length (Å) | 0.020 | | | |
| r.m.s. bond angles (deg.) | 2.7 | | | |
| No. atoms | | | | |
| Protein | 6419 | | | |
| Water | 155 | | | |
| Hetero | 471 | | | |
| Ramachandran plot[d] | | | | |
| Most favoured (%) | 89.9 | | | |
| Additionally allowed (%) | 9.8 | | | |
| Generously allowed (%) | 0.3 | | | |
| | Protein | Water | Hetero | Overall |
| Average *B*-factors | | | | |
| Main chain (Å$^2$) | 26.8 | | | 26.8 |
| Side-chain (Å$^2$) | 28.1 | | | 27.7 |
| All (Å$^2$) | 27.5 | 24.7 | 25.5 | 27.3 |

[a] Values in parentheses indicate statistics for the highest resolution shell.
[b] $R_{sym} = |\sum I_o - \langle I \rangle| / \sum I_o \times 100\%$, where $I_o$ is the observed intensity of reflection and $\langle I \rangle$ is the average intensity obtained from multiple observations of symmetry-related reflections.
[c] $R$-factor $= \| \Sigma F_o | - | F_c \| / | \Sigma F_o | \times 100\%$.
[d] By PROCHECK.

observe may, in some sense, correspond to a more "native-like" structure for the $Q_B$ tail at the protein/lipid interface *in vivo* relative to the orientation observed in detergent crystal structures.

### Automation of sponge phase crystallization

Steps towards the automation of the LCP crystallization methodology have been reported recently.[46,47] Although these developments have reduced the preparation time of the LCP and allow smaller volumes for crystallization setups, it is still more convenient to handle a liquid rather than a semi-solid LCP using standard crystallization robots, e.g. as in detergent-based protein crystallization setups. Since the sponge phase is a liquid, we repeated the crystallization experiments described above using a Cartesian honeybee robot (Genomic Solutions Ltd.) pipetted into a 96-well plate. Following this protocol, we obtained crystals, although they were significantly smaller than when using the hanging-drop, vapour-diffusion technique.

Since the major advantage of automation is that many crystallization experiments may be performed using only small amounts of purified protein, it is useful to reflect upon how sponge phase crystallization may be generalized towards a broad screen. In addition to this work showing that the RC crystallizes directly from a sponge phase recovered using an MO/jeffamine mixture, it has been established recently that a bacterial light-harvesting complex II crystallizes from the MO LCP *via* a sponge phase when adding PPO.[31] Other MO sponge phases can be accessed over a fairly broad temperature range and are relatively insensitive to both pH and ionic strength. For example, there exist MO sponge phases derived from the addition of: PEG 400,[28] PEG 600, PEG 1000, PEG 1500, PEG 3350, PEG 4000, PEG 8000 and PEG 20000[48] (typically 30% water, 30–65% PEG and 5–40% MO); NMP[30] (40% water, 20–55% NMP and 5–40% MO); MPD[32] (50–70% water, 7–18% MPD and 12–43% MO); DMSO (35% water, 35–60% DMSO and 5–30% MO); ethanol (60% water, 30% ethanol and 10% MO); PG[28] (40% water, 25–55% PG and 5–35% MO); butanediol (30–45%), jeffamine (12–20%); KSCN (1–2 M); PPO (14–22%); and t-butanol (12–20%).[31] Many of these additives are agents present in the traditional protein crystallization screen solutions, although some may induce protein denaturation at the concentrations required to generate a sponge phase. From this starting point, a screen consisting of 24, 48 or 96 crystallization conditions may easily be conceived using variations upon the sponge phases that have proven to give protein crystals (i.e. the jeffamine and PPO systems),[31] emphasizing the MO/PEG phases, using a smaller selection of other "mild" MO-based sponge phases, and spanning a broad range of pH and ionic strength, including both monovalent and divalent cations.[1] Once prepared and validated, the $L_3$ phase should be stable for many weeks (except at extreme pH, where MO may become hydrolysed) and vapour-diffusion crystallization experiments would proceed as described above. For reasons of expense, it may be convenient to prepare the reservoir solution lacking MO.

Alternatively, should a sponge phase be identified for which the protein of interest is stable, a convenient approach would be to premix the protein with this phase and then perform vapour diffusion experiments against commercially available crystallization screens. This is directly analogous to screening for crystallization conditions using the LCP, but with the advantage that the protein/MO system is liquid rather than semi-solid. In practice, one might use results from detergent crystallization screening to identify candidate $L_3$ phases in which the protein is likely to be stable (e.g. modify promising PEG conditions by adding MO at the correct ratio to create an $L_3$ phase) and thus sponge phase crystallization could be tried as a straightforward extension of promising, but not entirely satisfactory, earlier crystallization experiments. This establishes that, for screening experiments, only 100 nl of protein solution and 400 nl of $L_3$ phase are required, and therefore a far larger number of crystallization setups can be performed for any given quantity of purified protein.

## Conclusions

In this work, we show that crystals of RCsph can be grown in a liquid analogue of the cubic phase, i.e. the sponge phase. This liquid phase opens up new possibilities for a convenient approach to the

crystallization of membrane proteins in a native-like lipid environment. Sponge phases are not limited to jeffamine M600 and MO mixtures, but can be formed from PEG, PG, ethanol, MPD, DMSO, PPO, NMP, butanediol, KSCN, t-butanol and other reagents used frequently in protein crystallization screens. This implies that the approach described here could easily be generalized to incorporate many crystallization conditions.

Crystallization of a membrane protein from the LCP is suggested to start from a cubic Pn3m phase, to move through a cubic Ia3d phase, and end up in a lamellar $L_\alpha$ phase. In the case of RCsph, the LCP is transformed from Pn3m to Ia3d to $L_3$ and finally (presumably) to a l $L_\alpha$ phase. Here, we show that crystals from RCsph can be grown directly using the $L_3$ phase without needing to start from a cubic phase. The rationale behind our approach was to identify and characterize the phase transformation occurring during a membrane protein crystallization experiment. This led to a new approach (i.e. starting from the sponge phase), to larger and better-diffracting crystals with lower mosaic spread, and an improved electron density map in a functionally relevant part of the protein. Since phase transformations also frequently occur during detergent crystallization experiments, the rationale underpinning this approach could be extended to a generic crystallization procedure for other challenging problems in structural biology.

## Materials and Methods

The 1-mono-oleyl-*rac*-glycerol (MO) used for crystallization experiments was purchased from Sigma (99 % purity) and MO for phase studies was obtained from Danisco Cultor A/S (94.9 % purity; Brabrand, Denmark). The *N*,*N*-dimethyldodecylamine-*N*-oxide (LDAO) and 1,2,3-heptanetriol (high melting point isomer) were purchased from Fluka Chemika. Jeffamine M600 was purchased from Hampton Research. Deuterium oxide (99.8%) was obtained from Armar Chemicals (Döttingen, Switzerland).

### Sample preparation for the crystal violet experiment

MO and crystal violet solution (0.1 M Hepes (pH 8.1), 0.1 % (w/v) LDAO), containing a few crystals of crystal violet, were mixed in a ratio of 60:40 (w/w) until a viscous, violet and non-birefringent cubic phase was formed. The cubic phase was transferred to a glass vial and solution initiating sponge phase formation (1 M Hepes (pH 8.1), 20% jeffamine M600, 0.7 M $(NH_4)_2SO_4$ and 2.5% 1,2,3-heptanetriol) was added on top of the cubic phase in a ratio of 1 to 4 (v/v). Every hour a picture was taken over a period of 24 h until the cubic phase was dissolved completely.

### Sample preparation for phase studies

For the SAXS measurements, MO and 0.1 M Hepes (pH 8.1), 0.1 % (w/v) LDAO were mixed in a ratio of 60:40 (w/w) until a viscous, transparent and non-birefringent cubic phase was formed. The cubic phase was transferred to a 1 mm quartz capillary and sponge phase formation was initiated by adding 1 M Hepes (pH 8.1), 20% jeffamine M600, 0.7 M $(NH_4)_2SO_4$, 2.5% 1,2,3-heptanetriol to both sides of the cubic phase in a ratio of 1 to 4 (v/v). The small-angle scattering data were recorded on a Kratky camera (HECUS MBraun, Graz, Austria) with a position-sensitive detector, containing 1024 channels, each 55 μm wide. A monochromator with a nickel filter was used to select the Cu Kα radiation (λ = 1.542 Å) provided by an X-ray generator operated at 50 kV and 40 mA (Philips, PW 1830/40, The Netherlands). The temperature in the sample cell was regulated by a Peltier element (accuracy ± 0.1 deg. C), controlled by the software MTC version 4.2 (HECUS MBraun, Graz, Austria). The camera and the sample cell were held under vacuum to minimize the scatter from the air. Data were recorded with a sample detector distance of 282 mm. Scattering data were recorded each hour over period of 15 h and after three days the space group of the cubic crystalline phases were determined from prominent scattering peaks using the program 3Dview (HECUS MBraun, Graz, Austria).

The sample for the NMR experiment was prepared in a way similar to that used for the SAXS experiment. Initially, a cubic phase was prepared from MO and buffer in a ratio of 40:60 (w/w). Jeffamine solution (1 M Hepes (pH 8.1), 20% jeffamine M6000, 7 M $(NH_4)_2SO_4$, 2.5% 1,2,3-heptanetriol) was prepared using $^2H_2O$ instead of $^1H_2O$ and was added to the top of the cubic phase in a fourfold excess leading to an MO to jeffamine M600 ratio 1:1 (w/w). After complete phase separation at room temperature, the two liquid phases were separated and transferred to 5 mm NMR tubes. The phases were analysed by $^1H$ NMR ($^2H_2O$) spectra on a 400 MHz Varian Unity spectrometer and on a 600 MHz Varian Inova spectrometer.

### Protein crystallization in the sponge phase

Photosynthetic reaction centres from *R. sphaeroides* (strain R26) were prepared to a high purity of $A_{280}/A_{800} < 1.2$, as described.[49] The protein solution typically used for crystallization setups was concentrated to 20–25 mg/ml. After concentration, the buffer was exchanged to 0.1 M Hepes (pH 8.1), 0.1% LDAO. Sponge phases for protein crystallization were prepared from cubic MO/buffer phases, which were overlaid with a fourfold excess of crystallization agent solution. After equilibration and phase separation, the upper sponge phase was used as a precipitant solution in a hanging-drop, vapour-diffusion experiment. 4 μl of sponge phase was mixed with 1 μl of protein solution. This was equilibrated against a reservoir typically containing 1 M Hepes (pH 8.1), 20% jeffamine M600, 0.7 M $(NH_4)_2SO_4$. The crystallization experiments were carried out in the dark at room temperature.

### Protein crystallization in the sponge phase using the Cartesian honeybee robot

The sponge phase and the protein were prepared as described in the previous section. The Cartesian honeybee robot (Genomic Solutions Ltd.) was used to setup a sitting-drop experiment using 400 nl of sponge phase in a 96-well plate. Subsequently, 100 nl of protein solution was added on top of the sponge phase. The reservoir solution contained 1 M Hepes (pH 8.1), 20% jeffamine M600 and 0.7 M $(NH_4)_2SO_4$. The plate was sealed with crystal tape and stored in the dark at 20 °C. Crystals appeared after one week.

### Data collection and processing

Single-crystal X-ray data were collected at 100 K with an ADSC Q4 CCD detector at ID14-EH2 of the ESRF ($\lambda = 0.933$ Å). The oscillation range per image was 0.5°. Data were indexed and integrated with MOSFLM 6.2.4,[50] and scaled with SCALA 2.7.5,[51] of the CCP4 5.0.2 program suite.[52] The crystals belong to space group $P4_22_12$ with unit cell dimensions of $a = b = 100.4$ Å, $c = 235.4$ Å. Data statistics are summarized in Table 1.

### Model building and refinement

As starting model for the refinement, structure 1OGV was used,[6] water molecules were removed as well as cardiolipin. After rigid body refinement and simulated annealing using the program CNS 1.1,[53] rounds of manual rebuilding with O,[54] and crystallographic refinement with refmac5,[55] were alternated. 5% of the data were set apart for cross-validation and not used during refinement. Care was taken to select the test reflections that were used during refinement of 1OGV.[6] During the refinement, $Q_B$, one LDAO molecule and 155 water molecules werer modelled. Furthermore, the final model to 2.2 Å and *R*-factor 20.0% with $R_{free}$ of 24.6% consists of subunit H (residues 11–245), subunit L (residues 1–281), subunit M (residues 2–301), four bacteriochlorophylls, two bacteriopheophytins, one iron ion, one chloride ion and one more ubiquinone molecule. Simulated annealing omit maps omitting $Q_B$ were calculated using the program CNS 1.1.[53]

### Quality check and analysis of the final model

The quality and stereochemistry of the model were monitored during the refinement using the program PROCHECK,[56] and for structural analysis the program ESCET 0.9e was used.[42] For comparison of the $Q_B$ binding sites, the membrane-spanning part of all structures of RCsph were superimposed by superpose,[57] and Figures were produced with PyMOL‡.

### Protein Data Bank accession number

The crystallographic data and the refined model have been deposited at the Protein Data Bank with accession code 2GNU.

## Acknowledgements

We thank Paul Handa and Magnus Nydèn for measurements and discussions on the NMR samples, and Rob Horsefield for help with the Figures. We acknowledge experimental support from the staff of beamlines ESRF ID14 EH2 and EH4. We thank the Swedish Science Council (VR), the European Commission Improving Human Potential Program (FLASH), the European Commission Integrated Project EMEP, SWEGENE, and the Swedish Strategic Research Foundation (SSF) for financial support. GK acknowledges support from an EMBO long term fellowship.

‡ http://pymol.sourceforge.net/

## References

1. Iwata, S. (2002). *Methods & Results in Crystallization of Membrane Proteins.* International University Line, La Jolla, CA.
2. Landau, E. M. & Rosenbusch, J. P. (1996). Lipidic cubic phases: a novel concept for the crystallization of membrane proteins. *Proc. Natl Acad. Sci. USA*, **93**, 14532–14535.
3. Larsson, K. (1983). Two cubic phases in monoolein-water system. *Nature*, **304**, 664.
4. Longley, W. & McIntosh, T. J. (1983). A bicontinuous tetrahedral structure in a liquid-crystalline lipid. *Nature*, **303**, 612–614.
5. Lindblom, G., Larsson, K., Johansson, L., Fontell, K. & Forsen, S. (1979). The cubic phase of monoglyceride-water systems. Arguments for a structure based upon lamellar bilayer units. *J. Am. Chem. Soc.* **101**, 5465–5470.
6. Katona, G., Andreasson, U., Landau, E. M., Andreasson, L. E. & Neutze, R. (2003). Lipidic cubic phase crystal structure of the photosynthetic reaction centre from Rhodobacter sphaeroides at 2.35 Å resolution. *J. Mol. Biol.* **331**, 681–692.
7. Belrhali, H., Nollert, P., Royant, A., Menzel, C., Rosenbusch, J. P., Landau, E. M. & Pebay-Peyroula, E. (1999). Protein, lipid and water organization in bacteriorhodopsin crystals: a molecular view of the purple membrane at 1.9 Å resolution. *Structure*, **7**, 909–917.
8. Luecke, H., Schobert, B., Richter, H. T., Cartailler, J. P. & Lanyi, J. K. (1999). Structure of bacteriorhodopsin at 1.55 Å resolution. *J. Mol. Biol.* **291**, 899–911.
9. Pebay-Peyroula, E., Rummel, G., Rosenbusch, J. P. & Landau, E. M. (1997). X-ray structure of bacteriorhodopsin at 2.5 Å from microcrystals grown in lipidic cubic phases. *Science*, **277**, 1676–1681.
10. Kolbe, M., Besir, H., Essen, L. O. & Oesterhelt, D. (2000). Structure of the light-driven chloride pump halorhodopsin at 1.8 Å resolution. *Science*, **288**, 1390–1396.
11. Luecke, H., Schobert, B., Lanyi, J. K., Spudich, E. N. & Spudich, J. L. (2001). Crystal structure of sensory rhodopsin II at 2.4 Å: Insights into color tuning and transducer interaction. *Science*, **293**, 1499–1503.
12. Royant, A., Nollert, P., Edman, K., Neutze, R., Landau, E. M., Pebay-Peyroula, E. & Navarro, J. (2001). X-ray structure of sensory rhodopsin II at 2.1 Å resolution. *Proc. Natl Acad. Sci. USA*, **98**, 10131–10136.
13. Gordeliy, V. I., Labahn, J., Moukhametzianov, R., Efremov, R., Granzin, J., Schlesinger, R. *et al.* (2002). Molecular basis of transmembrane signalling by sensory rhodopsin II-transducer complex. *Nature*, **419**, 484–487.
14. Vogeley, L., Sineshchekov, O. A., Trivedi, V. D., Sasaki, J., Spudich, J. L. & Luecke, H. (2004). Anabaena sensory rhodopsin: a photochromic color sensor at 2.0 Å. *Science*, **306**, 1390–1393.
15. Chiu, M. L., Nollert, P., Loewen, M. C., Belrhali, H., Pebay-Peyroula, E., Rosenbusch, J. P. & Landau, E. M. (2000). Crystallization in cubo: general applicability to membrane proteins. *Acta. Crystallog. sect. D*, **56**, 781–784.
16. Misquitta, L. V., Misquitta, Y., Cherezov, V., Slattery, O., Mohan, J. M., Hart, D. *et al.* (2004). Membrane

protein crystallization in lipidic mesophases with tailored bilayers. *Structure*, **12**, 2113–2124.
17. Luecke, H., Schobert, B., Cartailler, J. P., Richter, H. T., Rosengarth, A., Needleman, R. & Lanyi, J. K. (2000). Coupling photoisomerization of retinal to directional transport in bacteriorhodopsin. *J. Mol. Biol.* **300**, 1237–1255.
18. Edman, K., Nollert, P., Royant, A., Belrhali, H., Pebay-Peyroula, E., Hajdu, J. *et al.* (1999). High-resolution X-ray structure of an early intermediate in the bacteriorhodopsin photocycle. *Nature*, **401**, 822–826.
19. Royant, A., Edman, K., Ursby, T., Pebay-Peyroula, E., Landau, E. M. & Neutze, R. (2000). Helix deformation is coupled to vectorial proton transport in the photocycle of bacteriorhodopsin. *Nature*, **406**, 645–648.
20. Neutze, R., Pebay-Peyroula, E., Edman, K., Royant, A., Navarro, J. & Landau, E. M. (2002). Bacteriorhodopsin: a high-resolution structural view of vectorial proton transport. *Biochim. Biophys. Acta*, **1565**, 144–167.
21. Luecke, H., Schobert, B., Richter, H. T., Cartailler, J. P. & Lanyi, J. K. (1999). Structural changes in bacteriorhodopsin during ion transport at 2 Å resolution. *Science*, **286**, 255–261.
22. Edman, K., Royant, A., Nollert, P., Maxwell, C. A., Pebay-Peyroula, E., Navarro, J. *et al.* (2002). Early structural rearrangements in the photocycle of an integral membrane sensory receptor. *Structure*, **10**, 473–482.
23. Moukhametzianov, R., Klare, J. P., Efremov, R., Baeken, C., Goeppner, A., Labahn, J., Engelhard, M., Bueldt, G. & Gordeliy, V. I. (2006). Development of the signal in sensory rhodopsin and its transfer to the cognate transducer. *Nature*, **440**, 115–119.
24. Katona, G., Snijder, A., Gourdon, P., Andreasson, U., Hansson, O., Andreasson, L. E. & Neutze, R. (2005). Conformational regulation of charge recombination reactions in a photosynthetic bacterial reaction center. *Nature Struct. Mol. Biol.* **12**, 630–631.
25. Nollert, P., Qiu, H., Caffrey, M., Rosenbusch, J. P. & Landau, E. M. (2001). Molecular mechanism for the crystallization of bacteriorhodopsin in lipidic cubic phases. *FEBS Letters*, **504**, 179–186.
26. Engblom, J., Miezis, Y., Nylander, T., Razumas, V. & Larsson, K. (2000). On the swelling of monoolein liquid-crystalline aqueous phases in the presence of distearoylphosphatidylglycerol. *Prog. Coll. Pol. Sci. S*, **116**, 9–15.
27. Sparr, E., Wadsten, P., Kocherbitov, V. & Engström, S. (2004). The effect of bacteriorhodopsin, detergent and hydration on the cubic-to-lamellar phase transition in the monoolein-distearoyl phosphatidyl glycerol-water system. *Biochim. Biophys. Acta*, **1665**, 156–166.
28. Engström, S., Alfons, K., Rasmusson, M. & Ljusberg-Wahren, H. (1998). Solvent-induced sponge ($L_3$) phases in the solvent-monoolein-water system. *Prog. Coll. Pol. Sci. S*, **108**, 93–98.
29. Evertsson, H., Stilbs, P., Lindblom, G. & Engström, S. (2002). NMR self diffusion measurements of the monooleoylglycerol/poly ethylene glycol/water L3 phase. *Colloid. Surface B*, **26**, 21–29.
30. Imberg, A., Evertsson, H., Stilbs, P., Kriechbaum, M. & Engström, S. (2003). On the self-assembly of monoolein in mixtures of water and a polar aprotic solvent. *J. Phys. Chem. B*, **107**, 2311–2318.
31. Cherezov, V., Clogston, J., Papiz, M. Z. & Caffrey, M. (2006). Room to move: crystallizing membrane proteins in swollen lipidic mesophases. *J. Mol. Biol.* **357**, 1605–1618.
32. Ridell, A., Ekelund, K., Evertsson, H. & Engström, S. (2003). On the water content of the solvent/monoolein/water sponge ($L_3$) phase. *Colloid. Surface A*, **228**, 17–23.
33. Cherezov, V., Fersi, H. & Caffrey, M. (2001). Crystallization screens: compatibility with the lipidic cubic phase for in meso crystallization of membrane proteins. *Biophys. J.* **81**, 225–242.
34. Caffrey, M. (2000). A lipid's eye view of membrane protein crystallization in mesophases. *Curr. Opin. Struct. Biol.* **10**, 486–497.
35. Faham, S. & Bowie, J. U. (2002). Bicelle crystallization: a new method for crystallizing membrane proteins yields a monomeric bacteriorhodopsin structure. *J. Mol. Biol.* **316**, 1–6.
36. Hiemenz, P. C. & Rajagopalan, R. (1997). *Principles of Colloid and Surface Chemistry*, 3rd edit. Marcel Dekker, New York.
37. Briggs, J., Chung, H. & Caffrey, M. (1996). The temperature-composition phase diagram and mesophase structure characterization of the monoolein/water system. *J. Phys. II*, **6**, 723–751.
38. Lei, N., Safinya, C. R., Roux, D. & Liang, K. S. (1997). Synchrotron X-ray-scattering studies on the sodium dodecyl sulfate-water-pentanol-dodecane L3 sponge phase. *Phys. Rev. E*, **56**, 608–613.
39. Gomati, R., Bouguerra, N. & Gharbi, A. (2001). Stability and swelling behaviour of a concentrated sponge phase. *Physica B*, **299**, 101–107.
40. Gotter, M., Strey, R., Olsson, U. & Wennerström, H. (2005). Fusion and fission of fluid amphiphhilic bilayers. *Faraday. Discuss.* **129**, 327–338.
41. Nollert, P. & Landau, E. M. (1998). Enzymatic release of crystals from lipidic cubic phases. *Biochem. Soc. Trans.* **26**, 709–713.
42. Schneider, T. R. (2002). A genetic algorithm for the identification of conformationally invariant regions in protein molecules. *Acta. Crystallog. sect. D*, **58**, 195–208.
43. Arnoux, B., Gaucher, J. F., Ducruix, A. & Reiss-Husson, F. (1995). Structure of the photochemical reaction centre of a spheroidene-containing purple-bacterium, Rhodobacter sphaeroides Y, at 3 Å resolution. *Acta. Crystallog. sect. D*, **51**, 368–379.
44. Roszak, A. W., McKendrick, K., Gardiner, A. T., Mitchell, I. A., Isaacs, N. W., Cogdell, R. J. *et al.* (2004). Protein regulation of carotenoid binding gatekeeper and locking amino acid residues in reaction centers of Rhodobacter sphaeroides. *Structure*, **12**, 765–773.
45. Stowell, M. H., McPhillips, T. M., Rees, D. C., Soltis, S. M., Abresch, E. & Feher, G. (1997). Light-induced structural changes in photosynthetic reaction center: implications for mechanism of electron-proton transfer. *Science*, **276**, 812–816.
46. Cherezov, V., Peddi, A., Muthusubramaniam, L., Zheng, Y. F. & Caffrey, M. (2004). A robotic system for crystallizing membrane and soluble proteins in lipidic mesophases. *Acta. Crystallog. sect. D*, **60**, 1795–1807.
47. Nollert, P. (2002). From test tube to plate: a simple procedure for the rapid preparation of microcrystallization experiments using the cubic phase method. *J. Appl. Crystallog.* **35**, 637–640.
48. Ridell, A. (2003). Characterisation of aqueous solutions, liquid crystals and solid state of non-ionic polymers in association with amphiphiles and drugs, thesis, Uppsala University.
49. Farhoosh, R., Chynwat, V., Gebhard, R., Lugtenburg, J. & Frank, H. A. (1997). Triplet energy transfer between the primary donor and carotenoids in

Rhodobacter sphaeroides R-26.1 reaction centers incorporated with spheroidene analogs having different extents of pi-electron conjugation. *Photoch. Photobio. Sci.* **66**, 97–104.
50. Steller, I., Bolotovsky, R. & Rossmann, M. G. (1997). An algorithm for automatic indexing of oscillation images using Fourier analysis. *J. Appl. Crystallog.* **30**, 1036–1040.
51. Kabsch, W. (1988). Evaluation of single-crystal X-ray diffraction data from a position-sensitive detector. *J. Appl. Crystallog.* **21**, 916–924.
52. Collaborative Computational Project Number 4. (1994). The CCP4 suite: programs for protein crystallography. *Acta. Crystallog. sect. D*, **50**, 760–763.
53. Brunger, A. T., Adams, P. D., Clore, G. M., DeLano, W. L., Gros, P., Grosse-Kunstleve, R. W. *et al.* (1998). Crystallography & NMR system: a new software suite for macromolecular structure determination. *Acta. Crystallog. sect. D*, **54**, 905–921.
54. Jones, T. A. & Kjeldgaard, M. (1997). Electron-density map interpretation. *Method. Enzymol.* **277**, 173–208.
55. Murshudov, G. N., Vagin, A. A. & Dodson, E. J. (1997). Refinement of macromolecular structures by the maximum-likelihood method. *Acta. Crystallog. sect. D*, **53**, 240–255.
56. Laskowski, R. A., MacArthur, M. W., Moss, D. S. & Thornton, J. M. (1993). PROCHECK: a program to check the stereochemical quality of protein structures. *J. Appl. Crystallog.* **26**, 283–291.
57. Krissinel, E. & Henrick, K. (2004). Secondary-structure matching (SSM), a new tool for fast protein structure alignment in three dimensions. *Acta. Crystallog. sect. D*, **60**, 2256–2268.

***Edited by I. Wilson***

*(Received 19 April 2006; received in revised form 15 June 2006; accepted 16 June 2006)*
Available online 7 July 2006